

Time-Constrained Erasure Correction for Data Recovery in UAV-Aided IoT

Kushwanth Sistu and Siddhartha S. Borkotoky

Abstract—We propose data-recovery schemes to improve the uplink reliability of Internet of Things (IoT) networks in which a gateway mounted on an unmanned aerial vehicle (UAV) collects data from sensor nodes on the ground. The proposed techniques employ fountain coding and message replication to correct frame erasures on the sensor-to-UAV links. A salient feature of the proposed schemes is their adaptive selection of the redundancy amount depending on the contact times between a sensor and the UAV. We illustrate our design philosophy for the special case of a network in which wake-up radios (WuRs) are used for activating the sensors upon the UAV's arrival, and the sensor-to-UAV data transfer employs the Long Range (LoRa) communication technology with random access.

Index Terms—IoT, UAV, Data Recovery, Erasure Correction

I. INTRODUCTION

UAVs as data aggregators in IoT networks can provide tremendous advantages in terms of device energy consumption, coverage, and flexibility [1]–[3]. In a typical UAV-aided IoT scenario, a gateway mounted on a UAV hovers over a cluster of sensors from time to time. The sensors transmit their messages to the UAV, which relays them over a high-capacity link to the sink. The messages may represent sensor readings of physical parameters [3], machine-learning model parameters for federated-learning applications [4], etc. Since sensor-to-UAV links are typically lossy due to low transmission power and interference [5], data-recovery mechanisms may be required on these links to meet the desired reliability levels of the IoT application.

Frame-level erasure-correction schemes such as message replication and fountain coding have been successfully used for data recovery in IoT networks. These approaches transmit redundant messages to compensate for lost messages. Their incorporation into UAV-aided IoT, however, requires additional considerations. For example, the limited hovering time of the UAV restricts the amount of redundant messages a sensor can transmit. Furthermore, since all sensors in a cluster compete for transmission times within the same UAV hovering window, excessive redundancy transmission may in fact be counterproductive due to increased collisions. These considerations must be incorporated into the design to effectively leverage the benefits of erasure correction in UAV-IoT. To our knowledge, existing literature lacks such studies, although prior work has demonstrated the reliability improvements offered by erasure coding when the contact time between a sensor and the data sink is short [6]. However, [6] does not consider the multipoint-to-point communication scenario that arises when

This work was supported by the Department of Science and Technology (DST), Government of India, through its Core Research Grant (CRG) No. CRG/2023/005803. The authors are with the School of Electrical and Computer Sciences, Indian Institute of Technology Bhubaneswar, Khordha 752050, India (e-mail: 20ee01042@iitbbs.ac.in, borkotoky@iitbbs.ac.in)

a UAV collects data from a sensor cluster, and the constraints imposed on a sensor's transmission policy by the potentially variable hovering time and the sensor's energy budget. Another approach toward improving the reliability of sensor-to-UAV message transfer is to eliminate frame collisions by using TDMA [7]. However, TDMA requires a reliable connection setup phase, in which the UAV learns which sensors wish to transmit and the size of their respective data and accordingly assigns time slots to each. Random access protocols avoid this requirement but increase collisions and losses.

To avoid the complexity of TDMA, this letter focuses on a random-access scenario amenable even to unsophisticated IoT nodes and develops methods for improving communication reliability. Specifically, we contribute the following:

- We devise two erasure-correction schemes to improve the reliability of message transfer from a cluster of sensors to a UAV gateway. One scheme employs fountain coding, and transmits redundant frames that are linear combinations of the sensor messages. The other scheme transmits message replicas. To our knowledge, this is the first investigation of this kind.
- Unlike conventional erasure correction, our schemes adaptively determine the amount of redundancy to be sent depending on the available contact time between the sender and the UAV. Consequently, they can adapt to scenarios where the UAV's hovering times are variable.
- We illustrate our design for a practical UAV-IoT setup in which the sensors and the UAV are equipped with wake-up radios (WuR) and Long Range (LoRa) transceivers.
- We develop analytical models for the schemes' performance to aid in system design.

II. SYSTEM MODEL

We consider a cluster of n sensors or end devices (EDs). Each ED contains a LoRa transceiver as the main radio. In addition, it has a WuR. During idle times, the EDs keep their main radio switched off to conserve power. The WuR, which consumes negligible power [8], is kept on at all times. The UAV occasionally visits the cluster and hovers above it for a certain duration. A sensor has β messages to send to the UAV within the hovering time. For channel access by the EDs, we employ the protocol of [9], which uses slotted communications from the EDs to the UAV with slot length T_s . The UAV hovers for N_s slots, numbered 0 through $N_s - 1$. At every slot beginning, the UAV broadcasts a wake-up call (WuC) whose data field contains the current slot number i and the value of N_s . Once awake, an ED transmits its messages to the UAV using one of the methods to be described in Section III. Since each WuC serves as a time reference, we do not assume

the use of additional synchronization mechanisms. However, techniques such as [10] may be employed if desired.

For every transmission on the ED-to-UAV uplink, one among N_f orthogonal frequency bands is chosen uniformly at random. Likewise, the spreading factor (SF) of the LoRa signal [11] is chosen uniformly at random from the set $\{7, 8, \dots, k_m\}$, where $7 \leq k_m \leq 12$. (The SF specifies the number of bits carried per LoRa modulation symbol. Commercial LoRa modules typically support SFs 7 through 12). We assume that a sensor is capable of transmitting a maximum of N_{\max} frames per data-collection cycle, where $N_{\max} > \beta$. Typically, the energy profile of a sensor determines N_{\max} . An example calculation of N_{\max} is given in Appendix A.

III. REDUNDANCY TRANSMISSION SCHEMES

Our schemes transmit up to $\beta + \varepsilon$ frames, where the design parameter $\varepsilon \leq N_{\max} - \beta$ represents the amount of redundancy sent for correcting frame erasures. We define $N(i) = N_s - i$ and $\gamma(i) = N(i) - \beta$. Thus, for an ED that wakes up in slot i , there are $N(i)$ slots remaining in the session, of which $\gamma(i)$ are available for redundancy transmission. Note that $\gamma(i)$ may be 0 or negative depending on the value of i . The two erasure-correction schemes operate as follows:

A. Fountain Coding

An ED first checks if there are enough slots available to transmit ε redundant frames, that is, whether $\gamma(i) \geq \varepsilon$.

If $\gamma(i) \geq \varepsilon$: The ED encodes the β source messages into $\beta + \varepsilon$ coded messages and transmits them over $\beta + \varepsilon$ randomly chosen slots out of the $N(i)$ available slots. Each coded message is a weighted linear combination of the source messages. For the random linear fountain code [12] used in our illustration, the j th coded message is given by $c_j = \sum_{l=0}^{\beta-1} \alpha_l^{(j)} \psi_l$, where ψ_l , $0 \leq l \leq \beta - 1$ denote the source messages and the coefficients $\alpha_l^{(j)}$ are chosen at random from a Galois field of a given order q (GF(q)). Upon receiving a set of z coded messages that contain β linearly independent combinations of the source messages, the receiver solves a system of linear equations (e.g., via Gaussian elimination) to obtain the source messages. By contrast, if fewer than β linearly independent combinations are received, then fountain decoding fails. The probability that fountain decoding succeeds upon receiving z coded messages is given by $P_{\text{dec}}(z) = \prod_{v=0}^{\beta-1} (1 - q^{v-z})$ for $z \geq \beta$, and 0 for $z < \beta$ [12].

If $\gamma(i) < \varepsilon$: Fountain coding is not applied. Instead, if $\beta \leq N(i)$, the β messages are transmitted over β randomly chosen slots. If $\beta > N(i)$, then the ED randomly selects $N(i)$ messages and sends them over the $N(i)$ slots. Messages not selected are discarded and deemed lost.

B. Message Replication

This scheme makes transmission decisions as follows:

$\gamma(i) \geq 0$: Let $\hat{\varepsilon}(i) = \min\{\gamma(i), \varepsilon\}$, and m_q and m_r be the quotient and the remainder, respectively, when $\hat{\varepsilon}(i)$ is divided by β . Each message is sent $m_q + 1$ times; further, m_r messages are randomly picked for one additional transmission.

$\gamma(i) < 0$: This implies $N(i) < \beta$. The ED randomly selects $N(i)$ messages and sends them over the $N(i)$ slots. Messages not selected are discarded and deemed lost.

IV. PERFORMANCE ANALYSIS

Let the *message delivery probability* denote the probability that an arbitrary message from an ED is delivered to the UAV. Let P_b be the probability that an ED successfully receives a WuC from the UAV. Then, the probability mass function for the slot in which an ED wakes up (denoted W) is

$$P_W(i) = (1 - P_b)^i P_b \quad (1)$$

for $0 \leq i \leq N_s - 1$, and 0 otherwise.

Lemma 1. *An ED that wakes up in slot i transmits a frame to the UAV in slot s with probability*

$$P_{\text{tx}}(s|W=i) = \begin{cases} (\beta + r)/N(i), & s \geq i, \gamma(i) \geq y \\ \min\{\beta/N(i), 1\}, & s \geq i, \gamma(i) < y \\ 0, & s < i, \end{cases} \quad (2)$$

where $r = y = \varepsilon$ for fountain coding and $r = \hat{\varepsilon}(i)$ and $y = 0$ for message replication.

Proof: First, consider fountain coding. By definition, the ED has $N(i)$ slots available for use. If $\gamma(i) \geq \varepsilon$, then $\beta + \varepsilon$ coded messages are randomly distributed over $N(i)$ slots; hence the probability of choosing a certain slot is $(\beta + \varepsilon)/N(i)$. If $\gamma(i) < \varepsilon$, then β uncoded messages are to be distributed over $N(i)$ slots; the probability of choosing a certain slot is either $\beta/N(i)$ (if $\beta \leq N(i)$), or 1 (if $\beta > N(i)$, meaning all slots are used and some messages are dropped.) This is succinctly expressed as $\min\{\beta/N(i), 1\}$. For message replication, the proof is identical, except that an ED transmits redundancy for any $\gamma(i) > 0$, and $\hat{\varepsilon}(i)$ is the number of redundant frames sent. ■

Let the *transmission success probability* (denoted $\zeta(s)$) be the probability that a frame sent in slot s is successfully received at the UAV. Consider such a frame F from an arbitrary ED E. Then $\zeta(s)$ is the probability that no other ED transmits in slot s using the same frequency band with enough received power to cause the loss of F. It can be determined as follows:

Lemma 2. *The probability that a given ED E' transmits a frame in a given slot s is*

$$P_{\text{col}}(s) = \sum_{j=0}^{\min\{N_s - \beta - y, s\}} \frac{\beta + r}{N(j)} P_W(j) + \theta_s \sum_{j=N_s - \beta - y + 1}^s \min\left\{\frac{\beta}{N(j)}, 1\right\} P_W(j), \quad (3)$$

where $r = y = \varepsilon$ for fountain coding, $r = \hat{\varepsilon}(i)$ and $y = 0$ for message replication, and

$$\theta_s = \begin{cases} 1, & s > N_s - \beta - y \\ 0, & \text{otherwise.} \end{cases} \quad (4)$$

Proof: We first consider fountain coding. Suppose E' wakes up in slot j . Then $\gamma(j) \geq \varepsilon$ if $j \leq N_s - \beta - \varepsilon$. From the argument in Lemma 1, the probability of selecting slot s in this case is $(\beta + \varepsilon)/N(j)$. The first term in (3) averages this probability over all j such that $\gamma(j) \geq \varepsilon$. The min operation in the upper limit of the summation ensures that we consider

only the values of j up to s (since an ED waking up after slot s cannot transmit in slot s .) Similarly, the second summation accounts for the transmission probabilities for all j such that $\gamma(j) < \varepsilon$. The multiplier θ_s ensures that we consider the second summation only when there exists a j that simultaneously satisfies both $\gamma(j) < \varepsilon$ and $j \leq s$.

For message replication, the proof is identical, except that an ED transmits redundancy for any $\gamma(i) > 0$, and $\hat{\varepsilon}(i)$ is the number of redundant frames sent. \blacksquare

To derive the transmission success probability, consider frame F from ED E and an interfering frame F' from ED E'. The probability that F and F' collide over the same channel is $P_{\text{col}}(s)\mathcal{F}/N_f$. Hence, the probability that one given ED (namely, E') enforces the loss of F is

$$\mathcal{L}(s) = P_{\text{col}}(s)\mathcal{F}/N_f. \quad (5)$$

where \mathcal{F} is the probability that F' is received with enough power to cause the loss of F. An expression for \mathcal{F} is derived in Appendix B for links with Nakagami- m fading, a common model for ground-to-UAV links [13]. Since there are $n-1$ potential interferers, the transmission success probability for F (using the strongest interferer model [11]) is

$$\zeta(s) = (1 - \mathcal{L}(s))^{n-1} = (1 - P_{\text{col}}(s)\mathcal{F}/N_f)^{n-1}. \quad (6)$$

A. Message-Delivery Probability for Fountain Coding

Consider an arbitrary message ψ from an arbitrary ED E that woke up in slot i . Then the following events can occur:

1) $\gamma(i) \geq \varepsilon$: In this case, E performs fountain coding and transmits $\beta + \varepsilon$ coded messages. Thus, the MDP for ψ is the probability that the received set of coded messages is decodable. The message delivery probability then becomes

$$\mathcal{S}_1(i) = \sum_{z=\beta}^{\beta+\varepsilon} \xi(z, i) P_{\text{dec}}(z) = \sum_{z=\beta}^{\beta+\varepsilon} \xi(z, i) \prod_{v=0}^{\beta-1} (1 - q^{v-z}), \quad (7)$$

where $\xi(z, i)$ is the probability that z out of the $\beta + \varepsilon$ transmissions are successful. Finding an exact expression for $\xi(z, i)$ is complicated due to the slot-dependent nature of the transmission success probability $\zeta(s)$. However, a fairly accurate approximation may be obtained by assuming that the transmission success events over different slots are mutually independent and have a fixed probability $\hat{\zeta}$, and then using the binomial mass function

$$\xi(z, i) \approx \binom{\beta + \varepsilon}{z} \hat{\zeta}^z (1 - \hat{\zeta})^{\beta + \varepsilon - z}. \quad (8)$$

The parameter $\hat{\zeta}$ is obtained by averaging the transmission success probabilities for the $N(i)$ slots that are available to the ED. That is

$$\hat{\zeta} = \frac{1}{N(i)} \sum_{s=i}^{N_s-1} \zeta(s). \quad (9)$$

2) $\gamma(i) < \varepsilon$: In this case, fountain coding is not performed, and the message ψ is sent as it is. The probability that ψ is sent over slot s is given by [9]

$$\mathcal{T}(s, i) = \frac{1}{N(i)} \min \left\{ \frac{N(i)}{\beta}, 1 \right\}, \quad i \leq s \leq N_s - 1. \quad (10)$$

The message delivery probability is thus

$$\mathcal{S}_2(i) = \sum_{s=i}^{N_s-1} \mathcal{T}(s, i) \zeta(s). \quad (11)$$

The overall message delivery probability is thus

$$\mathcal{S} = \sum_{i=0}^{N_s-\beta-\varepsilon} P_W(i) \mathcal{S}_1(i) + \sum_{i=N_s-\beta-\varepsilon+1}^{N_s-1} P_W(i) \mathcal{S}_2(i), \quad (12)$$

where the first summation is over those values of the wake-up instant i such that $\gamma(i) \geq \varepsilon$, and the second one is for $\gamma(i) < \varepsilon$.

B. Message-Delivery Probability for Message Replication

To derive the message delivery probability, consider an arbitrary message ψ from an arbitrary ED E. Suppose E wakes up in a slot i . Then the following events can occur:

1) $\gamma(i) > 0$: Of the β messages, $m_r(i)$ are sent $m_q(i)+1$ times, and the remaining $\beta - m_r(i)$ are sent $m_q(i)$ times. Thus, $\mathcal{P}_1(i) = (\beta - m_r(i))/\beta$ and $\mathcal{P}_2(i) = m_r(i)/\beta$ denote the probability that a given message is sent $m_q(i)$ times and $m_q(i)+1$ times, respectively. The corresponding probabilities that at least one copy of the message is delivered are approximately $1 - (1 - \hat{\zeta})^{m_q(i)}$ and $1 - (1 - \hat{\zeta})^{m_q(i)+1}$, where $\hat{\zeta}$ is defined as in (9).

$$\begin{aligned} \hat{\mathcal{S}}_1(i) &= \mathcal{P}_1(i) \left(1 - (1 - \hat{\zeta})^{m_q(i)} \right) \\ &\quad + \mathcal{P}_2(i) \left(1 - (1 - \hat{\zeta})^{m_q(i)+1} \right). \end{aligned} \quad (13)$$

2) $\gamma(i) \leq 0$: In this case, the probability that a given message is sent over slot s , and the subsequent message delivery probability are the same as in the fountain-coding scheme, and are given by (10) and (11), respectively.

Using a similar argument as used for (12), the overall message delivery probability for message replication is

$$\hat{\mathcal{S}} = \sum_{i=0}^{N_s-\beta} P_W(i) \hat{\mathcal{S}}_1(i) + \sum_{i=N_s-\beta+1}^{N_s-1} P_W(i) \hat{\mathcal{S}}_2(i), \quad (14)$$

where $\hat{\mathcal{S}}_2(i)$ is the same as $\mathcal{S}_2(i)$ given by (11).

V. NUMERICAL RESULTS

For simulations, we consider 30 EDs distributed over a circular region of 30 m radius, UAV altitude of 10 m, $\beta = 5$, $N_f = 8$, $q = 256$ for fountain coding, SF set $\{7, 8, 9\}$, and Nakagami- m fading with $m = 3$ and path-loss exponent 2.5. The simulations are performed in MATLAB. Every data point is obtained by averaging 10,000 simulation runs.

Fig. 1 shows the message delivery probabilities for $\varepsilon = 5$ as a function of the WuC reception probability P_b . For comparison, we show results for the random-access scheme of [9], which does not employ erasure correction. We also compare against a TDMA scheme similar to [7]. In [7], the UAV transmits a WuC when it arrives. EDs that successfully receive the WuC send joining requests through their main radios. The UAV assigns TDMA slots to the sensors from which it receives joining requests. Our evaluation of the TDMA benchmark considers the best-case scenario in which joining-request reception is always successful, that is, any device that receives the WuC

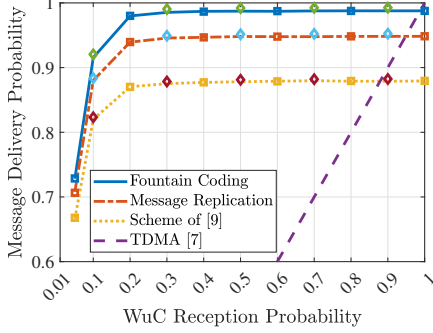


Fig. 1: Impact of WuC reception probability ($\varepsilon=5$, $N_s=30$). The lines show simulation results. Squares and diamonds show analytical results that utilize (22) and (24), respectively, in (6).

is allotted time slots. We observe that the proposed schemes consistently outperform [9], demonstrating the benefits of erasure correction. Also, fountain coding outperforms message replication due to the richer redundancy where every coded message carries information about all source messages as opposed to message replication carrying one source message per redundant frame. The TDMA scheme of [7] performs poorly when P_b is small (EDs often fail to wake up, and are hence not assigned transmission slots). Only for $P_b > 0.9$, TDMA performs better than the proposed schemes.

Fig. 2 shows the impact of UAV hovering time. In all cases, performance improves with hovering time, due to reduced collisions. For $\varepsilon = 3$, erasure correction schemes outperform [9]. For $\varepsilon=1$, message replication barely provides any improvement over [9], since it replicates only one out of the β messages, and thus only a loss of this message can be corrected. In addition, fountain coding performs much worse than other schemes when $N_s < 70$; this is because when $\varepsilon=1$, the set of coded messages is not decodable whenever there is more than a single erasure. For $N_s > 70$, frame losses become rarer, and fountain coding outperforms others. Thus, Fig. 2 illustrates the need for careful protocol selection depending on the redundancy budget and the available contact time.

Fig. 3 shows the impact of the number of EDs. Since collisions increase with node count, the performance of all scheme degrades. But with $\varepsilon = 3$, erasure correction outperforms [9], with fountain coding being significantly better. For $\varepsilon=1$, message replication performs virtually the same as the baseline, whereas fountain coding is worse than the baseline for high node densities (due to more frame losses leading to rank deficiency) and is better when there are fewer EDs.

VI. CONCLUSION

We described two erasure-correction schemes for data recovery in UAV-IoT data collection. We demonstrated their performance gains over existing approaches and identified how they are impacted by the UAV's hovering time, the maximum amount of redundancy transmission permitted by the sensor's energy budget, and device density. By improving the data-collection performance without a large complexity overhead, these schemes are expected to benefit a wide range of low-altitude UAV-IoT use cases such as precision agriculture and infrastructure monitoring.

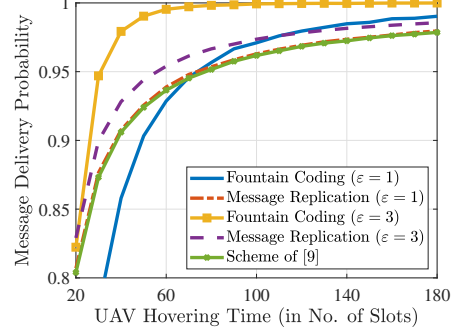


Fig. 2: Impact of UAV hovering time ($P_b=0.25$).

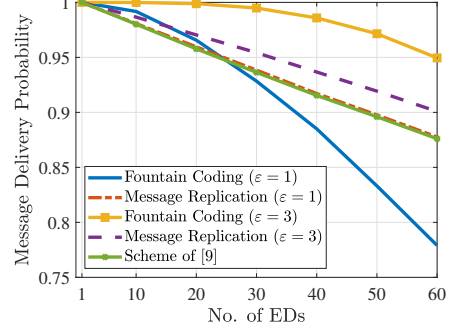


Fig. 3: Impact of node density n ($N_s=60$, $P_b=0.25$).

APPENDIX A

SENSOR TRANSMISSION LIMITS: EXAMPLE CALCULATION

Let $L_f(k)$ be the length of a LoRa frame using SF k . Thus, the average duration of a frame is $\bar{L}_f = \eta \sum_{k=7}^{K_m} L_f(k)$, where $\eta = 1/(k_m - 6)$ is the probability of choosing an SF. Let I_t be the current consumed by the main radio while transmitting, I_c be the device's current consumption while performing sensing-cum-computing tasks, and C_b be the battery capacity. Suppose that a device performs sensing and computational tasks for T_c seconds per day and the UAV visits the cluster V times per day. To ensure that the sensor battery lasts approximately L days, the number of frames N the sensor can transmit per UAV visit must satisfy

$$(N\bar{L}_f I_t V + T_c I_c)L \leq C_b. \quad (15)$$

The maximum possible value of N is therefore

$$N_{\max} = \left\lfloor \frac{C_b - LT_c I_c}{LV\bar{L}_f I_t} \right\rfloor. \quad (16)$$

For example, suppose $C_b = 600$ mAH, $L = 2$ years, $V = 12$, and $T_c = 20$ s, $k_m = 9$, and each message is 50 bytes. Assuming $I_t = 83$ mA [14] and $I_c = 50$ mA, we obtain $N_{\max} = 10$.

APPENDIX B

FRAME-LOSS PROBABILITY

We will assume that the EDs are uniformly distributed over a circular region with radius \mathcal{R} and the UAV is located h meters above the cluster center. Thus, the pdf for the distance D between an arbitrary ED and the UAV is

$$f_D(u) = \begin{cases} 2u/\mathcal{R}^2, & h \leq u \leq \sqrt{\mathcal{R}^2 + h^2} \\ 0, & \text{otherwise.} \end{cases} \quad (17)$$

and

$$f_D(u) = \begin{cases} 0, & u < h \\ (u^2 - h^2)/\mathcal{R}^2, & h \leq u \leq \sqrt{\mathcal{R}^2 + h^2} \\ 1, & \text{otherwise.} \end{cases} \quad (18)$$

Consider a frame F from an ED at distance d_0 . The power received at the UAV is $R = A\gamma_0 p_t d_0^{-\alpha}$, where p_t is the transmit power, α is the path-loss exponent, γ_0 is a hardware-dependent constant, and A is the power-fading coefficient. For Nakagami- m block fading, A is gamma distributed with its probability and cumulative distribution functions given by

$$f_A(a) = \frac{1}{\Gamma(m)} \left(\frac{m}{\Omega}\right)^m a^{m-1} e^{-\frac{ma}{\Omega}} \quad (19)$$

and

$$F_A(a) = \frac{1}{\Gamma(m)} \gamma\left(m, \frac{ma}{\Omega}\right), \quad a > 0, \quad (20)$$

respectively, where $\Omega = \mathbb{E}[A]$, $\Gamma(m) = \int_0^\infty t^{m-1} e^{-t} dt$, and $\gamma(m, x) = \int_0^x t^{m-1} e^{-t} dt$. Now consider a frame F' that collides with F on the same frequency channel. The received power in F' is $R' = \gamma_0 p_t A' u^{-\alpha}$, where A' is the fading coefficient and u is the distance to the UAV from the sender of F'. Let k and k' be the SFs used by F and F', respectively. Assuming the widely used strongest interferer model [11], F' causes a loss of F if $R/R' < \xi_{k,k'}$, where $\xi_{k,k'}$ is the capture threshold (see [15] for values). This occurs with probability

$$\begin{aligned} \tilde{\mathcal{F}} &= P(R/R' < \xi_{k,k'}) \\ &= P(ad_0^{-\alpha}/A'u^{-\alpha} < \xi_{k,k'}) \\ &= P(A' > \xi_{k,k'}^{-1} a(d_0/u)^{-\alpha}) \\ &= 1 - F_A(\xi_{k,k'}^{-1} a(d_0/u)^{-\alpha}) \\ &= 1 - \frac{1}{\Gamma(m)} \gamma\left(m, m\xi_{k,k'}^{-1} a(d_0/u)^{-\alpha}\right). \end{aligned} \quad (21)$$

Removing the conditioning on k , k' , a , d_0 , and u , we obtain

$$\mathcal{F} = \frac{1}{\eta^2} \sum_{k=7}^{k_m} \sum_{k'=7}^{k_m} \int_h^w \int_h^w \int_0^\infty \tilde{\mathcal{F}} f_A(a) f_D(d_0) f_D(u) da dd_0 du, \quad (22)$$

where $w = \sqrt{\mathcal{R}^2 + h^2}$ and $1/\eta^2 = 1/(k_m - 6)^2$ is the probability of choosing SFs k and k' , respectively, for the desired and colliding frames.

a) *A Closed-Form Approximation for \mathcal{F} :* A simple expression for \mathcal{F} can be derived by ignoring fading on the links, that is, letting $R = \gamma_0 p_t d_0^{-\alpha}$ and $R' = \gamma_0 p_t u^{-\alpha}$ and evaluating

$$\begin{aligned} \tilde{\mathcal{F}}(u) &\approx P(\gamma_0 p_t d_0^{-\alpha} / \gamma_0 p_t u^{-\alpha} < \xi_{k,k'}) \\ &= P(d_0 > \xi_{k,k'}^{-1/\alpha} u) \\ &= \begin{cases} 1, & u < \xi_{k,k'}^{1/\alpha} h \\ 1 - (\xi_{k,k'}^{-2/\alpha} u^2 - h^2)/\mathcal{R}^2, & \xi_{k,k'}^{1/\alpha} h \leq u \leq \xi_{k,k'}^{1/\alpha} w \\ 0, & u > \xi_{k,k'}^{1/\alpha} w, \end{cases} \end{aligned} \quad (23)$$

where $w = \sqrt{\mathcal{R}^2 + h^2}$. Removing the conditioning on k' , k , and u , we obtain the following approximation to (22)

$$\mathcal{F} \approx \frac{1}{\eta^2} \sum_{k=7}^{k_m} \sum_{k'=7}^{k_m} \int_h^w \tilde{\mathcal{F}}(u) f_D(u) du = \frac{1}{\eta^2} \sum_{k=7}^{k_m} \sum_{k'=7}^{k_m} I, \quad (24)$$

where the integral I evaluates to

$$I = \begin{cases} 0, & 0 < \xi_{k,k'}^{1/\alpha} < \frac{h}{w} \\ (b^2 - h^2)c - \xi_{k,k'}^{-2/\alpha}(b^4 - h^4), & \frac{h}{w} < \xi_{k,k'}^{1/\alpha} < 1 \\ \frac{a^2 - h^2}{\mathcal{R}^2} + (w^2 - h^2)c - \frac{\xi_{k,k'}^{-2/\alpha}}{2\mathcal{R}^2}(w^4 - a^4), & 1 < \xi_{k,k'}^{1/\alpha} < \frac{w}{h} \\ 1, & \frac{w}{h} < \xi_{k,k'}^{1/\alpha} < w, \end{cases} \quad (25)$$

where $a = \xi_{k,k'}^{1/\alpha} h$, $b = \xi_{k,k'}^{1/\alpha} w$, and $c = 1/\mathcal{R}^2 + h^2/\mathcal{R}^4$.

REFERENCES

- [1] H. K. Armeniakos, P. S. Bithas, K. Malatsos, and A. G. Kanatas, "Joint energy and SINR coverage probability in UAV corridor-assisted RF-powered IoT networks," *IEEE Communications Letters*, vol. 28, no. 12, pp. 2904–2908, 2024.
- [2] S. Zhang and R. Cao, "Multi-objective optimization for UAV-enabled wireless powered IoT networks: An LSTM-based deep reinforcement learning approach," *IEEE Communications Letters*, vol. 26, no. 12, pp. 3019–3023, 2022.
- [3] M. Bacco, A. Berton, A. Gotta, and L. Caviglione, "IEEE 802.15.4 air-ground UAV communications in smart farming scenarios," *IEEE Communications Letters*, vol. 22, no. 9, pp. 1910–1913, 2018.
- [4] D. C. Nguyen, M. Ding, P. N. Pathirana, A. Seneviratne, J. Li, and H. Vincent Poor, "Federated learning for Internet of Things: A comprehensive survey," *IEEE Communications Surveys & Tutorials*, vol. 23, no. 3, pp. 1622–1658, 2021.
- [5] Y. Xia, W. Liu, J. Xie, M. Xu, H. Li, Q. Zhang, C. Xu, S. Hu, and D. Huang, "Characterization of low-power wireless links in UAV-assisted wireless-sensor network," *IEEE Internet of Things Journal*, vol. 10, no. 7, pp. 5823–5842, 2023.
- [6] F. Dressler, M. Mutschlechner, B. Li, R. Kapitza, S. Ripperger, C. Eibel, B. Herzog, T. Hönig, and W. Schröder-Preikschat, "Monitoring bats in the wild: On using erasure codes for energy-efficient wireless sensor networks," *ACM Transactions on Sensor Networks (TOSN)*, vol. 12, no. 1, pp. 1–29, 2016.
- [7] S. L. Shah, Z. H. Abbas, G. Abbas, and N. H. Mahmood, "Energy-efficient and reliable data collection in receiver-initiated wake-up radio enabled IoT networks," *Computer Networks*, vol. 270, p. 111548, 2025.
- [8] R. Piyare, A. L. Murphy, C. Kiraly, P. Tosato, and D. Brunelli, "Ultra low power wake-up radios: A hardware and networking survey," *IEEE Communications Surveys & Tutorials*, vol. 19, no. 4, pp. 2117–2157, 2017.
- [9] S. M. S. Panga and S. S. Borkotoky, "Leveraging wake-up radios in UAV-aided LoRa networks: Some preliminary results on a random-access scheme," in *2023 17th International Conference on Telecommunications (ConTEL)*, pp. 1–7, 2023.
- [10] X. Huan, W. Chen, T. Wang, and H. Hu, "A microsecond energy-efficient LoRa time synchronization based on low-layer timestamping and asymmetric time translation," *IEEE Transactions on Vehicular Technology*, vol. 73, no. 5, pp. 7328–7332, 2024.
- [11] O. Georgiou and U. Raza, "Low power wide area network analysis: Can LoRa scale?," *IEEE Wireless Communications Letters*, vol. 6, no. 2, pp. 162–165, 2017.
- [12] E. Recayte, F. Lázaro, and G. Liva, "Caching in heterogeneous satellite networks with fountain codes," *International Journal of Satellite Communications and Networking*, vol. 40, no. 1, pp. 1–10, 2022.
- [13] L. Yuan, N. Yang, F. Fang, and Z. Ding, "Performance analysis of UAV-assisted short-packet cooperative communications," *IEEE Transactions on Vehicular Technology*, vol. 71, no. 4, pp. 4471–4476, 2022.
- [14] L. Casals, B. Mir, R. Vidal, and C. Gomez, "Modeling the energy performance of LoRaWAN," *Sensors*, vol. 17, no. 10, p. 2364, 2017.
- [15] A. Mahmood, E. Sisinni, L. Guntupalli, R. Rondón, S. A. Hassan, and M. Gidlund, "Scalability analysis of a LoRa network under imperfect orthogonality," *IEEE Transactions on Industrial Informatics*, vol. 15, no. 3, pp. 1425–1436, 2019.